INTERNATIONAL JOURNAL OF
ENERGY AND ENVIRONMENT

Volume 5, Issue 6, 2014 pp.655-668

Journal homepage: www.IJEE.IEEFoundation.org

Exergy analyses of an endoreversible closed regenerative Brayton cycle CCHP plant

Bo Yang[1,2,3], Lingen Chen[1,2,3], Yanlin Ge[1,2,3], Fengrui Sun[1,2,3]

[1] Institute of Thermal Science and Power Engineering, Naval University of Engineering, Wuhan 430033, P. R. China.
[2] Military Key Laboratory for Naval Ship Power Engineering, Naval University of Engineering, Wuhan 430033, P. R. China.
[3] College of Power Engineering, Naval University of Engineering, Wuhan 430033, P. R. China.

Abstract
An endoreversible closed regenerative Brayton cycle CCHP (combined cooling, heating and power) plant coupled to constant-temperature heat reservoirs is presented using finite time thermodynamics (FTT). The CCHP plant includes an endoreversible closed regenerative Brayton cycle, an endoreversible four-heat-reservoir absorption refrigerator and a heat recovery device of thermal consumer. The heat-resistance losses in the hot-, cold-, thermal consumer-, generator-, condenser-, evaporator- and absorber-side heat exchangers and regenerator are considered. The performance of the CCHP plant is studied from the exergetic perspective, and the analytical formulae about exergy output rate and exergy efficiency are derived. Through numerical calculations, the pressure ratio of regenerative Brayton cycle is optimized, the effects of heat conductance of regenerator and ratio of heat demanded by the thermal consumer to power output on dimensionless exergy output rate and exergy efficiency are analyzed.

Keywords: Finite time thermodynamics; Endoreversible closed regenerative Brayton cycle CCHP plant; Endoreversible four-heat-reservoir absorption refrigerator; Exergy output rate; Exergy efficiency.

1. Introduction

To solve energy crisis and reduce environmental pollution in the world, in recent years, people have paid much attention to new thermodynamic systems which are energy saving and environment friendly. Cogeneration which obeys energy cascade utilization principle is the simultaneous production of several forms of energy from one energy source. In general, cogeneration has two forms: CHP (combined heating and power) and CCHP (combined cooling, heating and power). Compared to conventional centralized cooling, heating or power generated systems, cogeneration has an advantage of high energy utilization efficiency and low emission of harmful pollution. Some researchers have studied CHP and CCHP plants using classical thermodynamics. Ertesvag [1] introduced relative avoided irreversibility (RAI) to analyze and compare the exergetic consequences of various legislations for CHP systems. Ferdelji *et al.* [2] performed exergy analysis (exergy losses and exergy efficiency) of a steam turbine CHP plant, and provided detailed information about magnitudes of losses and their distribution throughout the systems. Sanaye *et al.* [3] investigated the optimal design of a gas turbine CHP plant, defined an objective function as the sum of the operating cost related to the fuel consumption and the

capital investment for equipment purchase and maintenance costs. Khaliq and Dincer [4] investigated the energetic and exergetic performances of a CHP plant with absorption inlet cooling and evaporative aftercooling. Temir and Bilge [5] investigated the thermoeconomic performance of CCHP system taking investment and operation costs of the system into account. Mago and Chamra [6] evaluated and optimized the operation strategies of CCHP plant with considerations of primary energy consumption, operating costs and carbon dioxide emissions Khaliq [7] carried out the exergy analysis of a gas turbine CCHP system for combined production of power, heat and refrigeration. Kavvadias and Maroulis [8] developed a multi-objective optimization method for the design of CCHP plants considering technical, economical, energetic and environmental performance indicators.

Finite-time thermodynamics (FTT) [9-17] is a powerful tool for analyzing and optimizing performance of various thermodynamic cycles and devices. In recent years, some authors have carried out the performance analyses and optimization for various Brayton cycle CHP plants by using FTT. Yilmaz [18] optimized the exergy output rate and exergy efficiency of an endoreversible simple Brayton closed cycle CHP plant and found that the lower the consumer-side temperature, the better the exergy performance. Hao and Zhang [19, 20] optimized the total useful-energy rate (including power output and useful heat rate output) and the exergy output rate of an endoreversible Joule-Brayton CHP cycle by optimizing the pressure ratio. Ust *et al.* [21] introduced a new objective function called the exergetic performance coefficient (EPC), and optimized an irreversible regenerative Brayton closed cycle CHP plant with heat resistance and internal irreversibility. By using finite time exergoeconomic analysis [22-26], Tao *et al.* [27-29] performed the finite time exergoeconomic performance analyses and optimization for endoreversible simple [27] and regenerative [28] and irreversible simple [29] Brayton closed cycle CHP plants, and found that there existed an optimal heat consumer-side temperature through a new method of calculating thermal exergy output rate. Further, Chen *et al*. [30] and Yang *et al*. [31-34] investigated the finite time exergoeconomic performances of endoreversible constant-temperature heat reservoir [30, 31] and variable-temperature heat reservoir [32, 33] and irreversible constant-temperature heat reservoir [34] closed intercooled regenerative Brayton cycle CHP plants, respectively. Also Chen *et al*. [35] and Yang *et al*. [36] carried out performance analyses and optimization of exergy output rate and exergy efficiency for an endoreversible constant-temperature heat reservoir closed intercooled regenerative Brayton cycle CHP plant.

In the recent years, absorption refrigeration cycle which can be driven by 'low-grade' heat energy has attracted increasing attention, and some work on absorption refrigeration cycle using FTT has been developed. Chen [37] investigated the maximum specific cooling load of an irreversible four- heat-reservoir absorption refrigeration cycle with heat resistance and internal irreversibility by optimizing the distribution of the heat transfer areas of the heat exchangers. Chen *et al.* [38-40] and Zheng *et al.* [41-43] performed the cooling load and coefficient of performance (COP) performance analyses and optimization for endoreversible [38] and irreversible [39-43] four-heat-reservoir absorption refrigeration cycles with Newton's [39-41] and linear phenomenological [38, 42, 43] heat transfer laws. Qin *et al.* [44, 45] analyzed and optimized the thermoeconomic performance [44] and the cooling load and COP performance [45] of constant- temperature [44] and variable-temperature [45] four-heat-reservoir absorption refrigeration cycles. Tao *et al.* [46] studied the optimal ecological function performance of an endoreversible four-heat- reservoir absorption refrigeration cycle.

Using FTT, Chen *et al.* [47] and Feng *et al.* [48] established endoreversible [47] and irreversible [48] closed simple Brayton cycle CCHP plants which contain an endoreversible four- heat-reservoir absorption refrigerator, and performed finite time exergoeconomic performance optimization by optimizing the pressure ratio and the heat conductance distribution of the hot-, cold-, thermal consumer-, generator-, condenser-, evaporator- and absorber-side heat exchangers.

In the open literature, there is no work concerning FTT performance of regenerative Brayton cycle CCHP plant. Thus, in present study, an endoreversible regenerative Brayton cycle CCHP plant coupled to constant-temperature heat reservoirs is provided using FTT. The exergy output rate and exergy efficiency of the plant are investigated by optimizing pressure ratio of the regenerative Brayton cycle, and the effects of design parameters on the general and optimal performances are investigated by numerical calculation.

2. Thermodynamic model of the CCHP plant

Figure 1 shows the flow chart of an endoreversible closed regenerative Brayton cycle CCHP plant coupled to constant-temperature heat reservoirs. Figure 2 shows the *T*-*s* diagram. The whole cycle is

finished through the state changes of the working fluid. Process 1-2 is an isentropic adiabatic compression process in the compressor. Process 2-3 is an isobaric absorbed heat process in the regenerator. Process 3-4 is an isobaric absorbed heat process in the hot-side heat exchanger. Process 4-5 is isentropic adiabatic expansion process in the turbine. Process 5-6 is an isobaric evolved heat process in the regenerator. Process 6-7 is an isobaric supplied heat process in the generator-side heat exchanger. Process 7-8 is an isobaric supplied heat process in the thermal consumer-side heat exchanger. Process 8-1 is an isobaric evolved heat process in the cold-side heat exchanger.

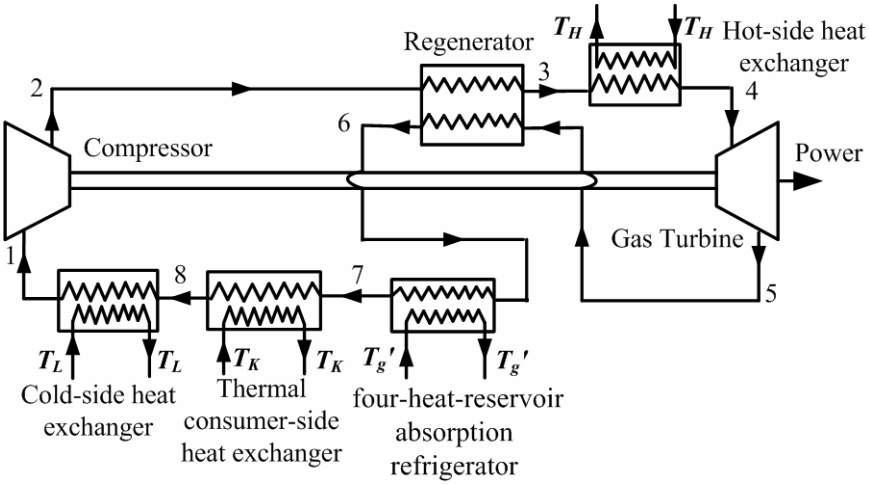

Figure 1. Schematic diagram of an endoreversible closed regenerative Brayton cycle CCHP plant

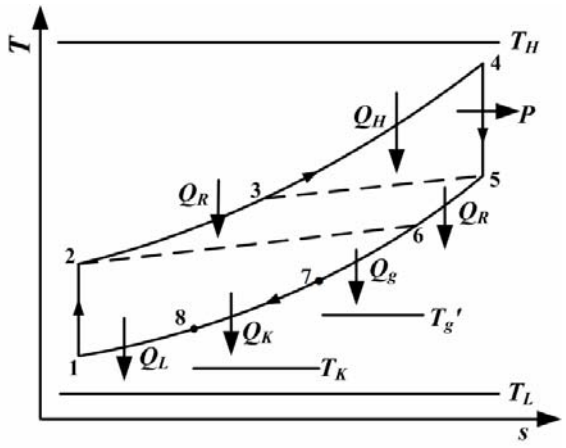

Figure 2. *T-s* diagram of an endoreversible closed regenerative Brayton cycle CCHP plant

Assuming that the working fluid used in the Brayton cycle is an ideal gas with constant thermal capacity rate C_{wf}. The hot-, cold- and thermal consumer-side heat reservoir temperatures are T_H, T_L and T_K respectively, and the temperature of working fluid in the generator is $T_g^{'}$. The heat exchangers between the working fluid and the heat reservoir and the regenerator are counter-flow. The heat conductances (heat transfer surface area and heat transfer coefficient product) of the hot-, cold-, generator- and thermal consumer-side heat exchangers, and the regenerator are U_H, U_L, U_g U_K, U_R respectively. Assuming that the heat transfer obeys a linear law, according to the properties of working fluid and the theory of heat exchangers, the heat transfer rate (Q_H) from the hot-side heat reservoir to the working fluid, the heat transfer rate (Q_L) from the working fluid to the cold-side heat reservoir, the heat transfer rate (Q_R) regenerated in the regenerator, the heat transfer rate (Q_g) from the working fluid of Brayton cycle to the working fluid in the generator, and the heat transfer rate (Q_K) from the working fluid of Brayton cycle to the thermal consumer device can be expressed as:

$$Q_H = C_{wf}(T_4 - T_3) = C_{wf} E_H (T_H - T_3) \tag{1}$$

$$Q_L = C_{wf}(T_8 - T_1) = C_{wf} E_L (T_8 - T_L) \tag{2}$$

$$Q_R = C_{wf}(T_3 - T_2) = C_{wf}(T_5 - T_6) = C_{wf} E_R (T_5 - T_2) \tag{3}$$

$$Q_g = C_{wf}(T_6 - T_7) = C_{wf} E_g (T_6 - T_g^{'}) \tag{4}$$

$$Q_K = C_{wf}(T_7 - T_8) = C_{wf} E_K (T_7 - T_K) \tag{5}$$

where E_H, E_L, E_R, E_g and E_K are the effectivenesses of the hot- and cold-side heat exchangers, the regenerator, the generator- and the thermal consumer-side heat exchanger respectively, which are used to reflect the heat resistance losses, and are defined as:

$$\begin{aligned} E_H &= 1-\exp(-N_H),\ E_L = 1-\exp(-N_L),\ E_R = 1-\exp(-N_R) \\ E_g &= 1-\exp(-N_g),\ E_K = 1-\exp(-N_K) \end{aligned} \tag{6}$$

where $N_i (i = H, L, R, g, K)$ are the numbers of heat transfer units of the hot- and cold-side heat exchangers, the regenerator, the generator- and the thermal consumer-side heat exchanger respectively, and are defined as:

$$N_H = U_H / C_{wf},\ N_L = U_L / C_{wf},\ N_R = U_R / C_{wf},\ N_g = U_g / C_{wf},\ N_K = U_K / C_{wf} \tag{7}$$

Defining that the pressure ratio of the regenerative Brayton cycle is π and the working fluid isentropic temperature ratio for the compression process 1-2 is y, i.e. $T_2 = yT_1$. According to the thermodynamic knowledge, one has:

$$T_4 = yT_5,\ y = \pi^{(k-1)/k} \tag{8}$$

where k is the specific heat ratio of the working fluid.

Figure 3 shows a model of an endoreversible four-heat-reservoir absorption refrigerator, which is composed of a generator, a condenser, an evaporator and an absorber. And there are four corresponding heat reservoirs, the temperature of the generator heat reservoir is variable, from T_6 to T_7, while the temperatures of the condenser, evaporator and absorber heat reservoir are constant, which are T_c, T_e and T_a, respectively. Assuming that the working fluid used in the absorption refrigerator flows steadily, and the temperatures of the working fluid in the condenser, evaporator and absorber are $T_c^{'}$, $T_e^{'}$ and $T_a^{'}$ respectively. The heat conductances of the condenser-, evaporator- and absorber-side heat exchanger are U_c, U_e and U_a, respectively. According to the theory of heat exchangers, the heat transfer rates (Q_c, Q_e and Q_a) which go through the condenser, evaporator and absorber can be, respectively, expressed as:

$$Q_c = U_c (T_c^{'} - T_c) \tag{9}$$

$$Q_e = R = U_e (T_e - T_e^{'}) \tag{10}$$

$$Q_a = U_a (T_a^{'} - T_a) \tag{11}$$

where R is the cooling load of the absorption refrigerator.

In addition, the power input required by the solution pump and heat loss rate caused by the flow of the working fluid in the absorption refrigerator can be negligible compared with the energy input to the generator. They are often neglected in the analyses and optimization of absorption refrigeration cycle

[37-48]. Therefore, the distribution ratio (n) of the total heat rejection between the absorber and condenser can be defined as:

$$n = Q_a / Q_c \tag{12}$$

For the endoreversible absorption refrigeration cycle, according to the first and second law of the thermodynamics, one has:

$$Q_g + Q_e - Q_a - Q_c = 0 \tag{13}$$

$$Q_g / T_g^{'} + Q_e / T_e^{'} - Q_a / T_a^{'} - Q_c / T_c^{'} = 0 \tag{14}$$

When U_c, U_e, U_a, T_c, T_e and T_a are fixed, combining equations (9)-(14), one can obtain the function relation between the cooling load (R) of the absorption refrigerator and the heat transfer rate (Q_g) that goes through the generator [37]:

$$\frac{Q_g}{T_g^{'}} + \frac{RU_e}{T_eU_e - R} - \frac{nU_a(Q_g + R)}{(n+1)T_aU_a + n(Q_g + R)} - \frac{U_c(Q_g + R)}{(n+1)T_cU_c + Q_g + R} = 0 \tag{15}$$

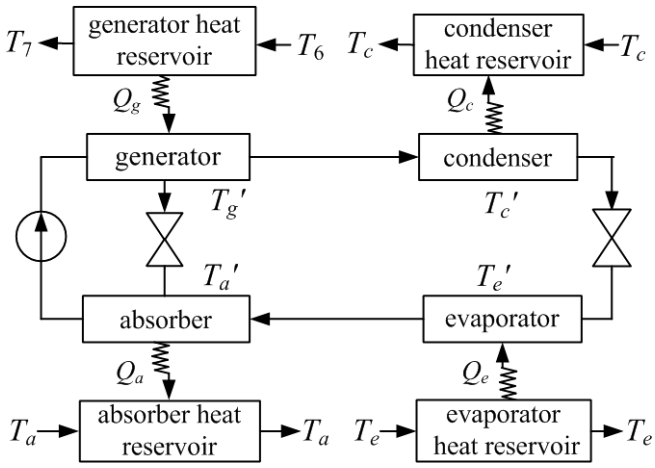

Figure 3. An endoreversible four-heat-reservoir absorption refrigerator model

3. Exergy performance analyses

According to the first law of thermodynamics, the power output (the exergy output rate of power) of the CCHP plant is:

$$P = Q_H - Q_L - Q_g - Q_K \tag{16}$$

The ratio of heat demanded by the thermal consumer to power output is defined as:

$$w = Q_K / P \tag{17}$$

Combining equations (1)-(5) with (8), (16) and (17) yields the temperatures (T_1, T_3, T_4, T_5, T_6, T_7, T_8, $T_g^{'}$) and the heat transfer rates (Q_H, Q_L, Q_R, Q_g and Q_K):

$$T_1 = \frac{wE_HT_H(y-1)(1-E_L)(1-E_K) - AE_K(E_LT_K - E_LT_L - T_K)}{AE_K - w(1-E_L)(1-E_K)[A - y^2E_H - y(1-E_H)(yE_R + 1 - 2E_R)]} \tag{18}$$

$$T_3 = \frac{y^2 T_1(1-E_R) + E_H E_R T_H}{A} \tag{19}$$

$$T_4 = \frac{yE_H T_H + y^2 T_1(1-E_H)(1-E_R)}{A} \tag{20}$$

$$T_5 = \frac{E_H T_H + yT_1(1-E_H)(1-E_R)}{A} \tag{21}$$

$$T_6 = \frac{(1-E_R)E_H T_H + yT_1[yE_R + (1-E_H)(1-2E_R)]}{A} \tag{22}$$

$$T_7 = \frac{T_1 - E_L T_L - E_K T_K + E_L E_K T_K}{(1-E_L)(1-E_K)} \tag{23}$$

$$T_8 = \frac{T_1 - E_L T_L}{1-E_L} \tag{24}$$

$$T_g^{'} = \frac{A(T_1 - E_L T_L - E_K T_K + E_L E_K T_K) - (1-E_L)(1-E_K)(1-E_g)\{(1-E_R)E_H T_H + yT_1[yE_R + (1-E_H)(1-2E_R)]\}}{AE_g(1-E_L)(1-E_K)} \tag{25}$$

$$Q_H = \frac{C_{wf} E_H[(y-E_R)T_H - y^2 T_1(1-E_R)]}{A} \tag{26}$$

$$Q_L = \frac{C_{wf} E_L(T_1 - T_L)}{1-E_L} \tag{27}$$

$$Q_R = \frac{C_{wf}[yT_1(y - yE_R - A) + E_H E_R T_H]}{A} \tag{28}$$

$$Q_g = \frac{C_{wf}(1-E_L)(1-E_K)\{(1-E_R)E_H T_H + yT_1[yE_R + (1-E_H)(1-2E_R)]\} - AC_{wf}(T_1 - E_L T_L - E_K T_K + E_L E_K T_K)}{A(1-E_L)(1-E_K)} \tag{29}$$

$$Q_K = \frac{C_{wf} E_K(T_1 + E_L T_K - T_K - E_L T_L)}{(1-E_L)(1-E_K)} \tag{30}$$

where $A = y - (1-E_H)E_R$.

Then the power output can be expressed as:

$$\begin{aligned} P &= Q_H - Q_L - Q_g - Q_K \\ &= C_{wf} E_H(1-E_L)(1-E_K)[(y-E_R)T_H - y^2 T_1(1-E_R)] - AC_{wf} E_L(T_1 - T_L)(1-E_K) - C_{wf}(1-E_L)(1-E_K)[y^2 E_R + (1-E_R)E_H T_H + yT_1(1-E_H)(1-2E_R)] + \\ &= \frac{AC_{wf}(T_1 - E_L T_L - E_K T_K + E_L E_K T_K) - AC_{wf} E_K(T_1 + T_K E_L - T_K - E_L T_L)}{A(1-E_L)(1-E_K)} \end{aligned} \tag{31}$$

Assuming that the ambient temperature is T_0, the net total exergy input rate of the CCHP plant is:

$$e_{in} = Q_H(1-T_0/T_H) - Q_L(1-T_0/T_L) \tag{32}$$

The thermal exergy output rate supplied for the thermal consumer is:

$$e_K = Q_K(1-T_0/T_K) = \frac{C_{wf}E_K(T_K-T_0)(T_1+T_KE_L-T_K-E_LT_L)}{(1-E_L)(1-E_K)T_K} \tag{33}$$

The cooling exergy output rate of the absorption refrigeration cycle is:

$$e_e = R(T_0/T_e-1) \tag{34}$$

where the cooling load (R) is decided by equations (15), (18), (25) and (29).
Applying the exergy conservation principle to the CCHP plant, one has:

$$e_{in} = P + e_K + e_e + T_0\sigma \tag{35}$$

Combining equations (26)-(35), the entropy generation rate (σ) of the CCHP plant can be yielded:

$$\begin{aligned}\sigma &= Q_L/T_L + Q_K/T_K + Q_g/T_0 + R(1/T_0-1/T_e) - Q_H/T_H \\ &= C_{wf}E_L(T_1-T_L)/[(1-E_L)T_L] + C_{wf}E_K(T_1+T_KE_L-T_K-E_LT_L)/[(1-E_L)\times \\ &\quad (1-E_K)T_K] + \{C_{wf}(1-E_L)(1-E_K)\{(1-E_R)E_HT_H + yT_1[yE_R+(1-E_H)(1- \\ &\quad 2E_R)]\} - AC_{wf}(T_1-E_LT_L-E_KT_K+E_LE_KT_K)\}/[AT_0(1-E_L)(1-E_K)] + \\ &\quad R(1/T_0-1/T_e) - C_{wf}E_H[(y-E_R)T_H - y^2T_1(1-E_R)]/(AT_H)\end{aligned} \tag{36}$$

The exergy output rate and exergy efficiency of the CCHP plant are defined as:

$$e_{out} = P + e_K + e_e \tag{37}$$

$$\eta_{ex} = e_{out}/e_{in} \tag{38}$$

Defining the nondimensionalized exergy output rate by using $C_{wf}T_0$:

$$\begin{aligned}\overline{e_{out}} &= (P+e_K+e_e)/(C_{wf}T_0) \\ &\quad T_KT_e\{C_{wf}E_H(1-E_L)(1-E_K)[(y-E_R)T_H - y^2T_1(1-E_R)] - AC_{wf}E_L(T_1- \\ &\quad T_L)(1-E_K) - C_{wf}(1-E_L)(1-E_K)[y^2E_R+(1-E_R)E_HT_H + yT_1(1-E_H)\times \\ &\quad (1-2E_R)] + AC_{wf}(T_1-E_LT_L-E_KT_K+E_LE_KT_K) - AC_{wf}E_K(T_1+T_KE_L- \\ &\quad T_K-E_LT_L)\} + AC_{wf}E_KT_e(T_K-T_0)(T_1+T_KE_L-T_K-E_LT_L) + ART_K\times \\ &= \frac{(T_0-T_e)(1-E_L)(1-E_K)}{AC_{wf}T_KT_eT_0(1-E_L)(1-E_K)}\end{aligned} \tag{39}$$

The exergy efficiency can be expressed as:

$$\eta_{ex} = \frac{P+e_K+e_e}{P+e_K+e_e+T_0\sigma} = 1 - \frac{\sigma}{\overline{e_{out}}C_{wf}+\sigma} \tag{40}$$

In addition, in order to make sure that the design state of the CCHP plant is meaningful, the power output (P), heat transfer rate (Q_g) supplied to the generator and heat transfer rate (Q_K) supplied to the thermal consumer device should be larger than zero, and the following equations about temperatures should be satisfied:

$$T_1 < T_2, T_3 < T_4, T_5 < T_4, T_7 < T_6, T_8 < T_7, T_1 < T_8 \tag{41}$$

4. Numerical examples

In order to see how the design parameters influence the dimensionless exergy output rate and exergy efficiency of the CCHP plant, detailed numerical examples are given. The following temperature ratios are defined: $\tau_H = T_H / T_0$, $\tau_L = T_L / T_0$, $\tau_K = T_K / T_0$, $\tau_e = T_e / T_0$. In the calculations, without special illustration, the numerical values of the parameters are set as follows: $k = 1.4$, $C_{wf} = 1.0kW / K$, $U_H = 2kW / K$, $U_L = 2kW / K$, $U_R = 2kW / K$, $U_K = 2kW / K$, $U_g = 2kW / K$, $U_c = 2kW / K$, $U_e = 2kW / K$, $U_a = 2kW / K$, $\tau_H = 5.0$, $\tau_L = 1$, $\tau_K = 1.2$, $T_c = 300K$, $T_e = 280K$, $T_a = 300K$, $T_0 = 300K$, $w = 0.4$, and $n = 1$.

4.1 Optimal pressure ratio

Figures 4 and 5 show the effects of U_R and w on the characteristics of $\overline{e_{out}}$ and η_{ex} versus π, respectively. It can be seen from Figure 4 that $\overline{e_{out}}$ and η_{ex} exist optimal values ($(\overline{e_{out}})_{opt}$ and $(\eta_{ex})_{opt}$) with respect to π respectively, and the corresponding optimal pressure ratios are notated as $\pi_{(\overline{e_{out}})_{opt}}$ and $\pi_{(\eta_{ex})_{opt}}$. A critical pressure ratio exists, and when π is smaller than the critical pressure ratio, the calculations indicate that $T_5 > T_2$ and $Q_R > 0$, thus $\overline{e_{out}}$ and η_{ex} increase with the increase of U_R; when π is larger than the critical pressure ratio, one has $T_5 < T_2$ and $Q_R < 0$, thus $\overline{e_{out}}$ and η_{ex} decrease with the increase of U_R, which is similar to the effect of regeneration on Brayton power cycle [49-51]. It can be seen from Figure 5 that $\overline{e_{out}}$ and η_{ex} increase equably with the increase of w. The broken lines in Figures 4 and 5 indicate that when U_R or w is large, and when π is smaller than certain values, one can obtain $T_6 < T_7$, $Q_g < 0$, which is shown in Figure 6, thus the CCHP plant becomes the CHP plant.

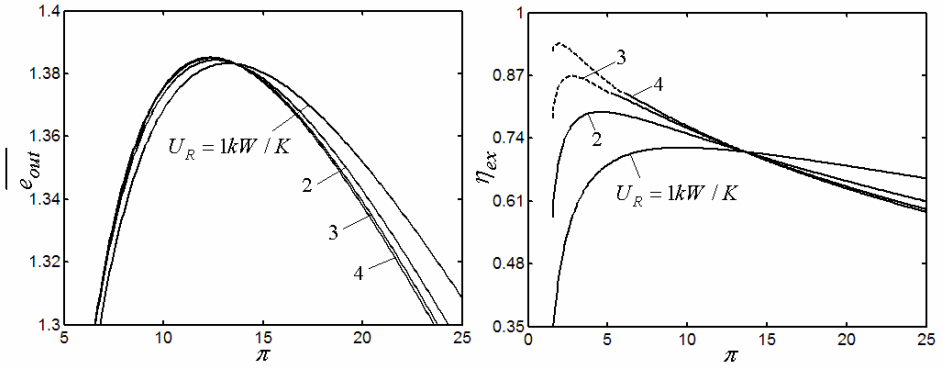

Figure 4. Effects of U_R on the characteristics of $\overline{e_{out}}$ and η_{ex} versus π

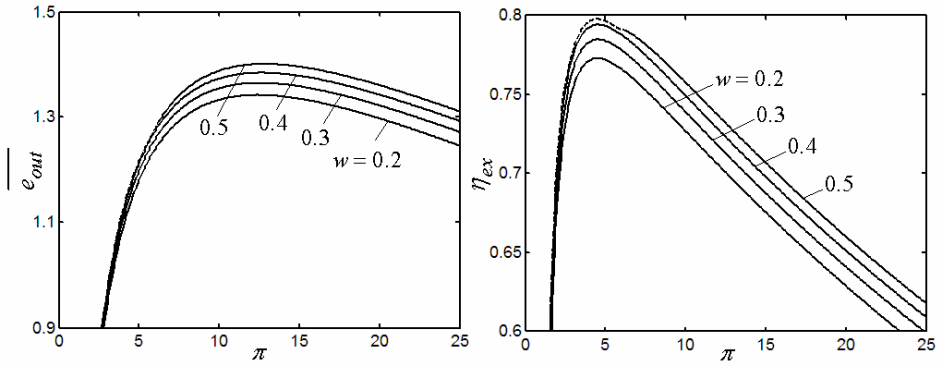

Figure 5. Effects of w on the characteristics of $\overline{e_{out}}$ and η_{ex} versus π

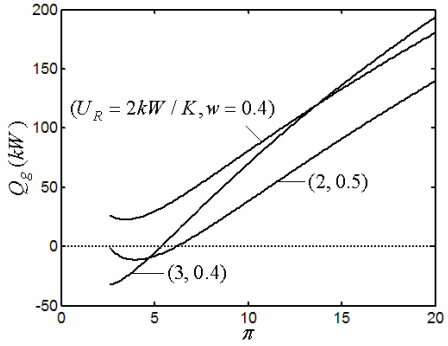

Figure 6. Relation of Q_g versus π for different U_R and w

4.2 Optimal dimensionless exergy output rate and optimal exergy efficiency

Figures 7-11 show the relations of the optimal dimensionless exergy output rate ($(\overline{e_{out}})_{opt}$) and corresponding exergy efficiency ($(\eta_{ex})_{(\overline{e_{out}})_{opt}}$), the optimal exergy efficiency ($(\eta_{ex})_{opt}$) and corresponding dimensionless exergy output rate ($(\overline{e_{out}})_{(\eta_{ex})_{opt}}$), and the two optimal pressure ratios ($\pi_{(\overline{e_{out}})_{opt}}$ and $\pi_{(\eta_{ex})_{opt}}$, which correspond to $(\overline{e_{out}})_{opt}$ and $(\eta_{ex})_{opt}$) versus τ_H, U_H, τ_e, $U_g = U_c = U_e = U_a$ and τ_K, respectively.

It can be seen from Figure 7 that $(\overline{e_{out}})_{opt}$, $(\overline{e_{out}})_{(\eta_{ex})_{opt}}$, $(\eta_{ex})_{opt}$, $(\eta_{ex})_{(\overline{e_{out}})_{opt}}$, $\pi_{(\overline{e_{out}})_{opt}}$ and $\pi_{(\eta_{ex})_{opt}}$ increase monotonically with the increase of τ_H, and one has $(\overline{e_{out}})_{opt} > (\overline{e_{out}})_{(\eta_{ex})_{opt}}$, $(\eta_{ex})_{opt} > (\eta_{ex})_{(\overline{e_{out}})_{opt}}$ and $\pi_{(\overline{e_{out}})_{opt}} > \pi_{(\eta_{ex})_{opt}}$ for the same τ_H, which indicates that the optimal design scope of the CCHP plant should be $(\overline{e_{out}})_{(\eta_{ex})_{opt}} < \overline{e_{out}} < (\overline{e_{out}})_{opt}$, $(\eta_{ex})_{(\overline{e_{out}})_{opt}} < \eta_{ex} < (\eta_{ex})_{opt}$. It also can be seen that with the increase of τ_H, the range $[\pi_{(\eta_{ex})_{opt}}, \pi_{(\overline{e_{out}})_{opt}}]$ expands.

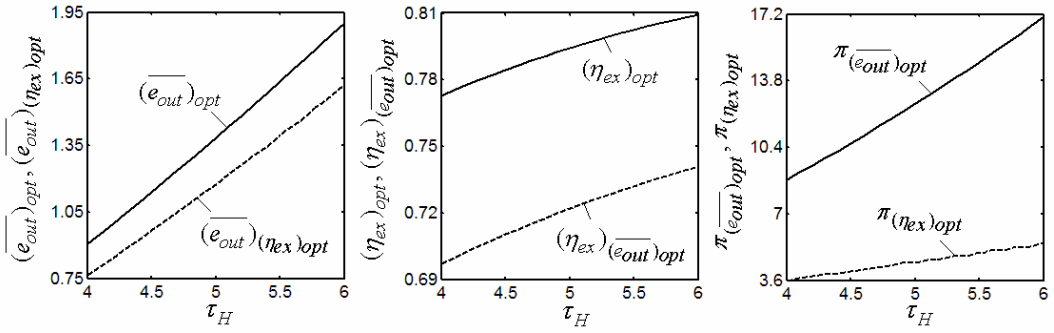

Figure 7. Relations of $(\overline{e_{out}})_{opt}$, $(\overline{e_{out}})_{(\eta_{ex})_{opt}}$, $(\eta_{ex})_{opt}$, $(\eta_{ex})_{(\overline{e_{out}})_{opt}}$, $\pi_{(\overline{e_{out}})_{opt}}$, and $\pi_{(\eta_{ex})_{opt}}$ versus τ_H

It can be seen from Figure 8 that $(\overline{e_{out}})_{opt}$, $(\overline{e_{out}})_{(\eta_{ex})_{opt}}$, $(\eta_{ex})_{opt}$, $(\eta_{ex})_{(\overline{e_{out}})_{opt}}$, $\pi_{(\overline{e_{out}})_{opt}}$ and $\pi_{(\eta_{ex})_{opt}}$ increase with the increase of U_H, and increase slowly when U_H is large. The calculations also indicate that the influences of U_L and U_K on the exergy performances of the CCHP plant are similar to U_H.

It can be seen from Figure 9 that $(\overline{e_{out}})_{opt}$, $(\overline{e_{out}})_{(\eta_{ex})_{opt}}$, $(\eta_{ex})_{opt}$, $(\eta_{ex})_{(\overline{e_{out}})_{opt}}$, $\pi_{(\overline{e_{out}})_{opt}}$ and $\pi_{(\eta_{ex})_{opt}}$ decrease nearly linearly with the increase of τ_e.

It can be seen from Figure 10 that $(\overline{e_{out}})_{opt}$, $(\overline{e_{out}})_{(\eta_{ex})_{opt}}$, $(\eta_{ex})_{opt}$, $(\eta_{ex})_{(\overline{e_{out}})_{opt}}$, $\pi_{(\overline{e_{out}})_{opt}}$ and $\pi_{(\eta_{ex})_{opt}}$ increase with the increase of $U_g = U_c = U_e = U_a$, but the variations of the numerical values are slight.

It can be seen from Figure 11 that with the increase of τ_K, $(\overline{e_{out}})_{opt}$ and $(\eta_{ex})_{(\overline{e_{out}})_{opt}}$ increase first and then decrease, i.e. there exists an optimal value of thermal consumer-side temperature which makes $(\overline{e_{out}})_{opt}$

reach a maximum dimensionless exergy output rate. For $(\eta_{ex})_{opt}$, the calculations indicate that when τ_K is increased to a certain value (about 1.3 in this example), the heat transfer rate is smaller than zero, i.e. $Q_g < 0$, thus in a meaningful design range of τ_K, $(\eta_{ex})_{opt}$ and $(\overline{e_{out}})_{(\eta_{ex})_{opt}}$ increase with the increase of τ_K. It also can be seen from Figure 11 that with the increase of τ_K, $\pi_{(\overline{e_{out}})_{opt}}$ decreases first and then increases, and the change of $\pi_{(\eta_{ex})_{opt}}$ is not obviously.

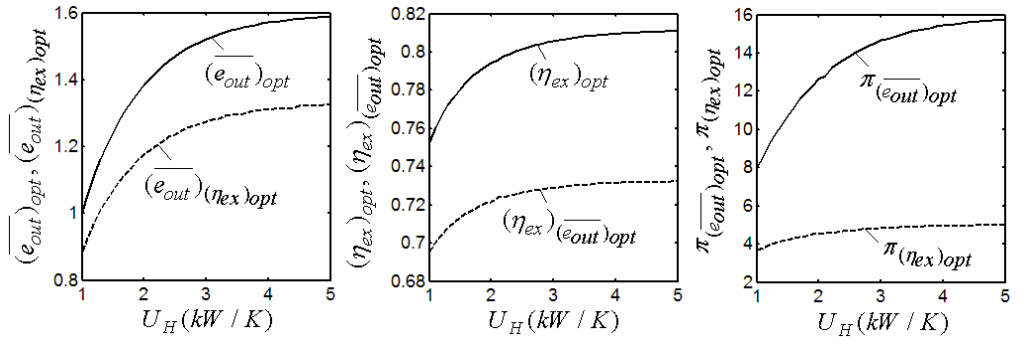

Figure 8. Relations of $(\overline{e_{out}})_{opt}$, $(\overline{e_{out}})_{(\eta_{ex})_{opt}}$, $(\eta_{ex})_{opt}$, $(\eta_{ex})_{(\overline{e_{out}})_{opt}}$, $\pi_{(\overline{e_{out}})_{opt}}$, and $\pi_{(\eta_{ex})_{opt}}$ versus U_H

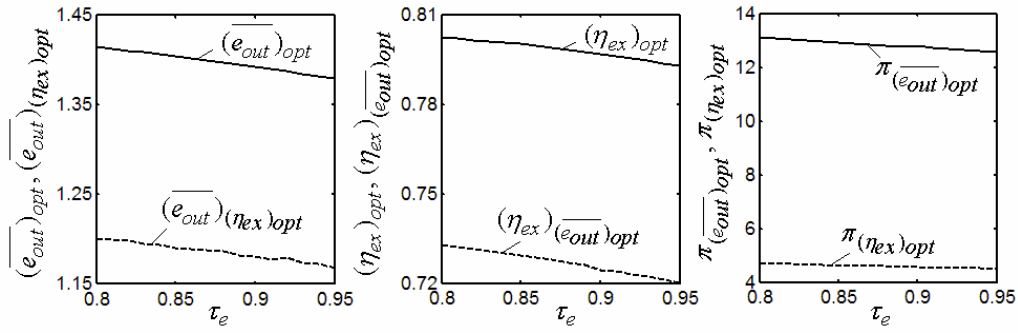

Figure 9. Relations of $(\overline{e_{out}})_{opt}$, $(\overline{e_{out}})_{(\eta_{ex})_{opt}}$, $(\eta_{ex})_{opt}$, $(\eta_{ex})_{(\overline{e_{out}})_{opt}}$, $\pi_{(\overline{e_{out}})_{opt}}$, and $\pi_{(\eta_{ex})_{opt}}$ versus τ_e

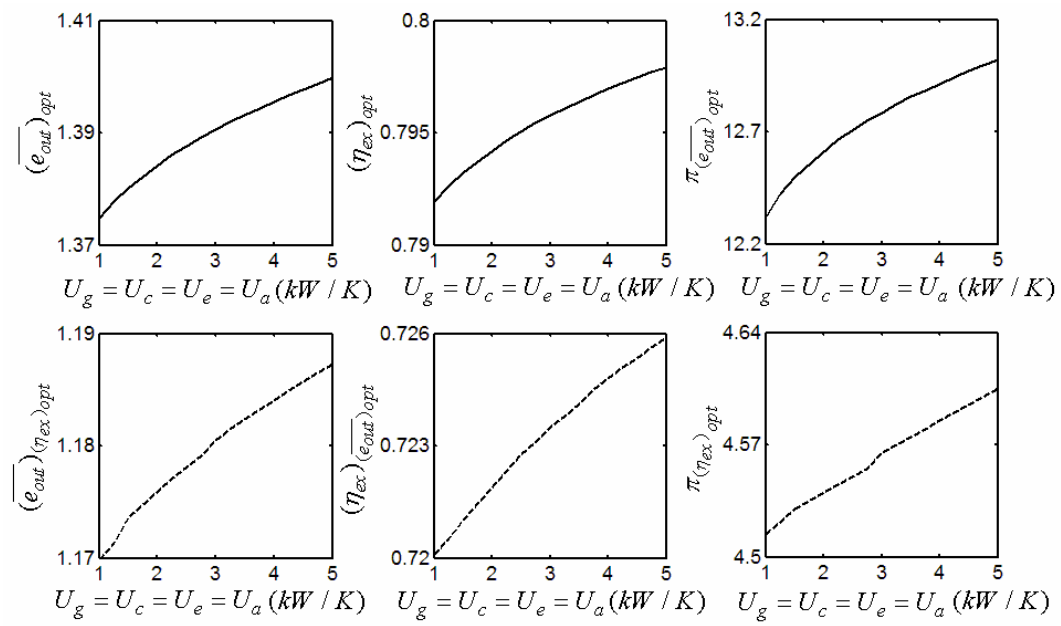

Figure 10. Relations of $(\overline{e_{out}})_{opt}$, $(\overline{e_{out}})_{(\eta_{ex})_{opt}}$, $(\eta_{ex})_{opt}$, $(\eta_{ex})_{(\overline{e_{out}})_{opt}}$, $\pi_{(\overline{e_{out}})_{opt}}$, and $\pi_{(\eta_{ex})_{opt}}$ versus $U_g = U_c = U_e = U_a$

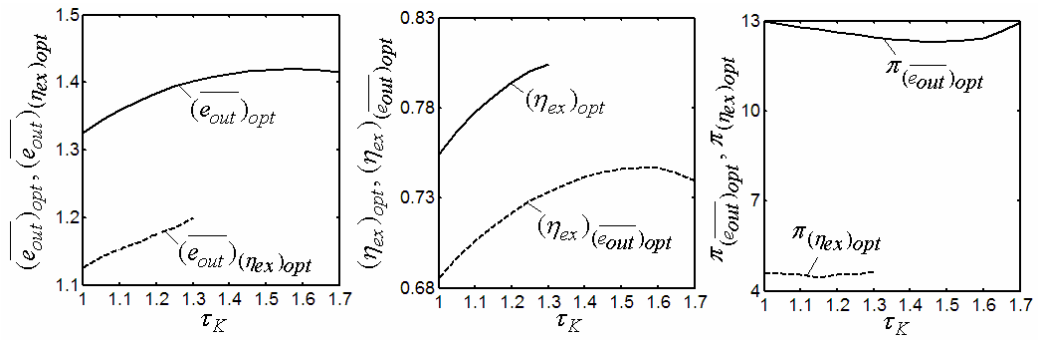

Figure 11. Relations of $(\overline{e_{out}})_{opt}$, $(\overline{e_{out}})_{(\eta_{ex})_{opt}}$, $(\eta_{ex})_{opt}$, $(\eta_{ex})_{(\overline{e_{out}})_{opt}}$, $\pi_{(\overline{e_{out}})_{opt}}$, and $\pi_{(\eta_{ex})_{opt}}$ versus τ_K

5. Conclusion

In present work, FTT is used to establish a CCHP plant model composed of an endoreversible closed regenerative Brayton cycle, an endoreversible four-heat-reservoir absorption refrigerator and a heat recovery device of thermal consumer. The exergy output rate and exergy efficiency of the plant are researched by theoretical analyses and numerical calculations, and the significant results are as follows:

(1) Both dimensionless exergy output rate and exergy efficiency have optimal values with respect to the pressure ratio of regenerative Brayton cycle. For regeneration, a critical pressure ratio exists, when pressure ratio is smaller than the critical pressure ratio, dimensionless exergy output rate and exergy efficiency increase with the increase of heat conductance of regenerator, and when pressure ratio is larger than the critical pressure ratio, dimensionless exergy output rate and exergy efficiency decrease with the increase of heat conductance of regenerator.

(2) The larger the ratio of heat demanded by the thermal consumer to power output of the plant, the better the exergy performances. But when the heat to power output ratio or the heat conductance of regenerator is too large and the pressure ratio is smaller than certain value, the CCHP plant will become a CHP plant.

(3) The appropriate design scope of the CCHP plant is determined by four paramters (optimal dimensionless exergy output rate and corresponding exergy efficiency, as well as optimal exergy efficiency and corresponding dimensionless exergy output rate). The optimal exergy performances can be further improved by increasing the ratio of hot-side heat reservoir temperature to environment temperature, the heat conductances of the hot-, cold- and thermal consumer-side heat exchangers, and decreasing the ratio of evaporator heat reservoir temperature to environment temperature. The influences of the heat conductances of the generator-, condenser-, evaporator- and absorber-side heat exchanger on the exergy performances are slight.

(4) The optimal dimensionless exergy output rate has a maximum with respect to the thermal consumer temperature, and in a meaningful design range, exergy efficiency increases with the increase of thermal consumer temperature.

The investigation in this paper may provide some guidelines for the optimal design and parameters selection of practical Brayton cycle CCHP plant.

Acknowledgments

This paper is supported by the National Key Basic Research and Development Program of China (973) (Project No. 2012CB720405) and The National Natural Science Foundation of P. R. China (Project No. 10905093).

Nomenclature

C	heat capacity rate (kW / K)	τ_L	ratio of cold-side heat reservoir temperature to environment temperature
E	effectiveness of the heat exchanger	τ_K	ratio of thermal consumer-side temperature to environment temperature
e	exergy flow rate (kW)	***Subscripts***	
k	ratio of the specific heats	a	absorber
N	number of heat transfer units	c	condenser
n	distribution ratio of heat rejection between absorber and condenser	e	evaporator

P	power output of the CCHP plant (kW)	ex	exergy
Q	rate of heat transfer (kW)	g	generator
R	cooling load of the absorption refrigerator (kW)	H	hot-side
T	temperature (K)	in	input
U	heat conductance (kW / K)	K	thermal consumer-side
w	ratio of heat demanded by the thermal consumer to power output	L	cold-side
y	isentropic temperature ratio for compression process or expansion process	opt	optimal
Greek symbols		out	output
η	efficiency	R	regenerator
π	pressure ratio	wf	working fluid
σ	entropy generation rate of the CCHP plant (kW / K)	0	ambient
τ_e	ratio of evaporator heat reservoir temperature to environment temperature	$1, 2, 3, 4, 5, 6, 7, 8$	state points of the cycle
τ_H	ratio of hot-side heat reservoir temperature to environment temperature	–	dimensionless

References

[1] Ertesvag I S. Exergetic comparison of efficiency indicators for combined heat and power (CHP). Energy, 2007, 32(11): 2038-2050.

[2] Ferdelji N, Galovic A , Guzovic Z. Exergy analysis of a co-generation plant. Therm. Sci., 2008, 12(4): 75-88.

[3] Sanaye S, Ziabasharhagh M and Ghazinejad M. Optimal design of gas turbine CHP plant with preheater and HRSG. Int. J. Energy Res., 2009, 39(8): 766-777.

[4] Khaliq A, Dincer I. Energetic and exergetic performance analyses of a combined heat and power plant with absorption inlet cooling and evaporative aftercooling. Energy, 2011, 36(5): 2662-2670.

[5] Temir G, Bilge D. Thermoeconomic analysis of a trigeneration system. Appl. Therm. Eng., 2004, 24(17/18): 2689-2699.

[6] Mago P J, Chamra L M. Analysis and optimization of CCHP systems based on energy, economical, and environmental considerations. Energy & Buildings, 2009, 41(10): 1099-1106.

[7] Khaliq A. Exergy analysis of gas turbine trigeneration system for combined production of power heat and refrigeration. Int. J. Refri., 2009, 32(3): 534-545.

[8] Kavvadias K C, Maroulis Z B. Multi-objective optimization of a trigeneration plant. Energy Policy, 2010, 38(2): 945-954.

[9] Bejan A. Entropy generation minimization: The new thermodynamics of finite-size devices and finite-time process. J. Appl. Phys., 1996, 79(3): 1191-1218.

[10] Hoffmann K H, Burzler J M, Schubert S. Endoreversible thermodynamics. J. Non-Equilib. Thermodyn., 1997, 22(4): 311-355.

[11] Berry R S, Kazakov V A, Sieniutycz S, Szwast Z, Tsirlin A M. Thermodynamic Optimization of Finite Time Processes. Chichester: Wiley, 1999.

[12] Chen L, Wu C, Sun F. Finite time thermodynamic optimization of entropy generation minimization of energy systems. J. Non-Equilib. Thermodyn., 1999, 24(4): 327-359.

[13] Chen L, Sun F. Advances in Finite Time Thermodynamics: Analysis and Optimization. New York: Nova Science Publishers, 2004.

[14] De Vos A. Thermodynamics of Solar Energy Conversion. Berlin: Wiley-Vch, 2008.

[15] Sieniutycz S, Jezowski J. Energy Optimization in Process Systems. Elsevier, Oxford, UK, 2009.

[16] Andresen B. Current trends in finite-time thermodynamics. Angew. Chem. Int. Ed., 2011, 50(12): 2690-2704.

[17] Feidt M. Thermodynamics of energy systems and processes: A review and perspectives. J. Appl. Fluid Mechanics, 2012, 5(2): 85-98.

[18] Yilmaz T. Performance optimization of a gas turbine-based cogeneration system. J. Phys. D: Appl. Phys., 2006, 39(11): 2454-2458.

[19] Hao X, Zhang G. Maximum useful energy-rate analysis of an endoreversible Joule-Brayton cogeneration cycle. Appl. Energy, 2007, 84(11): 1092-1101.

[20] Hao X, Zhang G. Exergy optimisation of a Brayton cycle-based cogeneration plant. Int. J. Exergy, 2009, 6(1): 34-48.
[21] Ust Y, Sahin B, Yilmaz T. Optimization of a regenerative gas-turbine cogeneration system based on a new exergetic performance criterion: exergetic performance coefficient. Proc. IMechE, Part A: J. Power Energy, 2007, 221(4): 447-458.
[22] Chen L, Sun F, Chen W. Finite time exergoeconomic performance bound and optimization criteria for two-heat-reservoir refrigerators. Chin. Sci. Bull., 1991, 36(2): 156-157 (in Chinese).
[23] Wu C, Chen L, Sun F. Effect of heat transfer law on finite time exergoeconomic performance of heat engines. Energy, 1996, 21(12): 1127-1134.
[24] Chen L, Sun F, Wu C. Exergoeconomic performance bound and optimization criteria for heat engines. Int. J. Ambient Energy, 1997, 18(4): 216-218.
[25] Wu C, Chen L, Sun F. Effect of heat transfer law on finite time exergoeconomic performance of a Carnot heat pump. Energy Convers. Mgmt., 1998, 39(7): 579-588.
[26] Chen L, Wu C, Sun F. Effect of heat transfer law on finite time exergoeconomic performance of a Carnot refrigerator. Int. J. Exergy, 2001, 1(4): 295-302.
[27] Tao G, Chen L, Sun F, Wu C. Exergoeconomic performance optimization for an endoreversible simple gas turbine closed-cycle cogeneration plant. Int. J. Ambient Energy, 2009, 30(3): 115-124.
[28] Tao G, Chen L, Sun F. Exergoeconomic performance optimization for an endoreversible regenerative gas turbine closed-cycle cogeneration plant. Rev. Mex. Fis., 2009, 55(3): 192-200.
[29] Chen L, Tao G, Sun F. Finite time exergoeconomic optimal performance for an irreversible gas turbine closed-cycle cogeneration plant. Int. J. Sustainable Energy, 2012, 31(1): 43-58.
[30] Chen L, Yang B, Sun F. Exergoeconomic performance optimization of an endoreversible intercooled regenerated Brayton cogeneration plant. Part 1: thermodynamic model and parameter analyses. Int. J. Energy & Environment, 2011, 2(2): 199-210.
[31] Yang B, Chen L, Sun F. Exergoeconomic performance optimization of an endoreversible intercooled regenerated Brayton cogeneration plant. Part 2: heat conductance allocation and pressure ratio optimization. Int. J. Energy & Environment, 2011, 2(2): 211-218.
[32] Yang B, Chen L, Sun F. Exergoeconomic performance analyses of an endreversible intercooled regenerative Brayton cogeneration type model. Int. J. Sustainable Energy, 2011, 30(2): 65-81.
[33] Yang B, Chen L, Sun F. Exergoeconomic performance optimization of an endoreversible intercooled regenerative Brayton combined heat and power plant coupled to variable- temperature heat reservoirs. Int. J. Energy & Environment, 2012, 3(4): 505-520.
[34] Yang B, Chen L, Sun F. Finite time exergoeconomic performance of an irreversible intercooled regenerative Brayton cogeneration plant. J. Energy Inst., 2011, 84(1): 5-12.
[35] Chen L, Yang B, Sun F, Wu C. Exergetic performance optimisation of an endoreversible intercooled regenerated Brayton cogeneration plant. Part 1: thermodynamic model and parametric analysis. Int. J. Ambient Energy, 2011, 32(3): 116-123.
[36] Yang B, Chen L, Sun F, Wu C. Exergetic performance optimisation of an endoreversible intercooled regenerated Brayton cogeneration plant. Part 2: exergy output rate and exergy efficiency optimisation. Int. J. Ambient Energy, 2012, 33(2): 98-104.
[37] Chen J. The optimum performance characteristics of a four-temperature-lever irreversible absorption refrigerator at maximum specific cooling load. J. Phys. D: Appl. Phys., 1999, 32(24): 3085-3091.
[38] Chen L, Zheng T, Sun F, Wu C. Optimal cooling load and COP relationship of a four-heat-reservoir endoreversible absorption refrigerator cycle. Entropy, 2004, 6(3): 316-326.
[39] Chen L, Zheng T, Sun F, Wu C. Performance limits of real absorption refrigerators. J. Energy Inst., 2005, 78(3): 139-144.
[40] Chen L, Zheng T, Sun F, Wu C. Irreversible four-temperature-level absorption refrigerator. Sol. Energy, 2006, 80(3): 347-360.
[41] Zheng T, Chen L, Sun F, Wu C. Performance of a four-heat-reservoir absorption refrigerator with heat resistance and heat leak. Int. J. Ambient Energy, 2003, 24(3): 157-168.
[42] Zheng T, Chen L, Sun F, Wu C. Performance optimization of an irreversible four-heat- reservoir absorption refrigerator. Appl. Energy, 2003, 76(4): 391-414.
[43] Zheng T, Chen L, Sun F, Wu C. The influence of heat resistance and heat leak on the performance of a four-heat-reservoir absorption refrigerator with heat transfer law of $Q \propto \Delta(T^{-1})$, Int. J. Therm. Sci., 2004, 43(12): 1187-1195.

[44] Qin X, Chen L, Sun F Wu C. Thermoeconomic optimization of an endoreversible four-heat-reservoir absorption-refrigerator. Appl. Energy, 2005, 81(4): 420-433.
[45] Qin X, Chen L, Sun F. Thermodynamic modeling and performance of variable-temperature heat reservoir absorption refrigeration cycle. Int. J. Exergy, 2010, 7(4): 521-534.
[46] Tao G, Chen L, Sun F, Wu C. Optimization between cooling load and entropy-generation rate of an endoreversible four-heat-reservoir absorption refrigerator. Int. J. Ambient Energy, 2009, 30(1): 27-32.
[47] Chen L, Feng H, Sun F. Exergoeconomic performance optimization for a combined cooling, heating and power generation plant with an endoreversible closed Brayton cycle. Math. Compu. Model., 2011, 54(11-12): 2785-2801.
[48] Feng H, Chen L, Sun F. Exergoeconomic optimal performance of an irreversible closed Brayton cycle combined cooling, heating and power plant. Appl. Math. Model., 2011, 35(9): 4661-4673.
[49] Wu C, Chen L, Sun F. Performance of a regenerating Brayton heat engines. Energy, 1996, 21(2): 71-76.
[50] Chen L, Sun F, Wu C. Theoretical analysis of the performance of a regenerated closed Brayton cycle with internal irreversibilities. Energy Convers. Manage., 1997, 38(9): 871-877.
[51] Chen L, Sun F, Wu C. Optimum heat conductance distribution for power optimization of a regenerated closed Brayton cycle. Int. J. Green Energy, 2005, 2(3): 243-258.

Bo Yang received his BS Degree in 2008 and MS Degree in 2010 from the Naval University of Engineering, P R China. He is pursuing for his PhD Degree in power engineering and engineering thermophysics from Naval University of Engineering, P R China. His work covers topics in finite time thermodynamics and technology support for propulsion plants. Dr Yang is the author or coauthor of 36 peer-refereed articles (12 in English journals).

Lingen Chen received all his degrees (BS, 1983; MS, 1986, PhD, 1998) in power engineering and engineering thermophysics from the Naval University of Engineering, P R China. His work covers a diversity of topics in engineering thermodynamics, constructal theory, turbomachinery, reliability engineering, and technology support for propulsion plants. He had been the Director of the Department of Nuclear Energy Science and Engineering, the Superintendent of the Postgraduate School, and the President of the College of Naval Architecture and Power. Now, he is the Direct, Institute of Thermal Science and Power Engineering, the Director, Military Key Laboratory for Naval Ship Power Engineering, and the President of the College of Power Engineering, Naval University of Engineering, P R China. Professor Chen is the author or co-author of over 1400 peer-refereed articles (over 620 in English journals) and nine books (two in English).
E-mail address: lgchenna@yahoo.com; lingenchen@hotmail.com, Fax: 0086-27-83638709 Tel: 0086-27-83615046.

Yanlin Ge received all his degrees (BS, 2002; MS, 2005, PhD, 2011) in power engineering and engineering thermophysics from the Naval University of Engineering, P R China. His work covers topics in finite time thermodynamics and technology support for propulsion plants. Dr Ge is the author or coauthor of over 90 peer-refereed articles (over 40 in English journals).

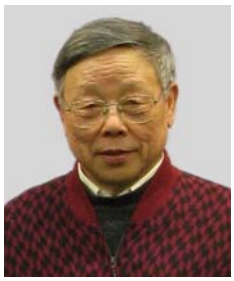

Fengrui Sun received his BS Degrees in 1958 in Power Engineering from the Harbing University of Technology, P R China. His work covers a diversity of topics in engineering thermodynamics, constructal theory, reliability engineering, and marine nuclear reactor engineering. He is a Professor in the College of Power Engineering, Naval University of Engineering, P R China. Professor Sun is the author or co-author of over 850 peer-refereed papers (over 440 in English) and two books (one in English).

